On Spatiochromatic Features in Natural Images Statistics

Edoardo Provenzi[1(✉)], Julie Delon[1], Yann Gousseau[2], and Baptiste Mazin[2]

[1] Sorbonne Paris Cité, Laboratoire MAP5, UMR CNRS 8145, Université Paris Descartes, 45 rue des Saints Pères, 75006 Paris, France
edoardo.provenzi@parisdescartes.fr

[2] Télécom ParisTech, LTCI, CNRS, 46, rue Barrault, 75013 Paris, France

Abstract. In this communication, we show that two simple assumptions on the covariances matrices of color images, namely stationarity and commutativity, can explain the observed shape of decorrelated spatiochromatic elements (bases obtained by PCA) of natural color images. The validity of these assumptions is tested on a large database of RAW images. Our experiments also show that the spatiochromatic covariance decays exponentially with the spatial distance between pairs of pixels and not as a power law as it is commonly assumed.

1 Introduction

Two kind of redundancies characterize the interaction between humans and natural scenes: the spatial one, due to the fact that nearby points are likely to send similar radiance information to the eyes (unless they lie in the proximity of a sharp edge), and the chromatic one, implied by the overlapping of the spectral sensitivity functions $L(\lambda), M(\lambda), S(\lambda)$ of retinal cones. *Spatio-chromatic correlation* is the term used to define both effects at once.

While there is a large literature on opponent color spaces and it is also known that spatial stationarity imply the appearance of *Fourier-like structure* in the Principal Component Analysis (PCA), the spatio-chromatic structure of color images has been less studied. One of the most striking known empirical observation is that the spatio-chromatic covariance matrices resemble a tensor product between a Fourier basis and color opponent channels, as pointed out in section 2.

In this work, we focus on this statistical characteristic, both from a theoretical and an experimental perspective, proving that two simple assumptions on the nature of spatiochromatic covariance matrices of real-world images are enough to explain the appearance of the tensor product structure.

In this communication, due to space bounds, we will only discuss tests performed on a database of RAW images. Further results on a large database of compressed images, coherent with those obtained with RAW images, can be found in [9]. A longer and more complete version has been submitted to Vision Research.

V. Murino and E. Puppo (Eds.): ICIAP 2015, Part II, LNCS 9280, pp. 46–55, 2015.
DOI: 10.1007/978-3-319-23234-8_5

Known results of second order statistics between pixel values are the *Fourier-like structure* of Principal Component Analysis (PCA), a result of *spatial stationarity*, and the *power-law decay* of the covariance, as a possible consequence of *scale-invariance*. Higher order statistics have also been largely investigated, for instance through wavelets or sparse coding.

On the other hand, several works have been concerned with chromatic redundancy in images, mostly through second order property and in connection with opponent color spaces.

However, the spatio-chromatic structure of color images has been less studied. One of the most striking known empirical observation is that the spatio-chromatic covariance matrices resemble a tensor product between a Fourier basis and color opponent channels, as pointed out in section 2.

In this work, we focus on this statistical characteristic, both from a theoretical and an experimental perspective, proving that two simple assumptions on the nature of spatiochromatic covariance matrices of real-world images are enough to explain the reason for the appearance of the tensor product structure.

In order to have a better perspective on this result, we will first start by recalling the most relevant results of second order natural image statistics related to this work.

2 Previous Studies on Spatial and Chromatic Natural Color Image Statistics

The literature about natural image statistics is vast and its exhaustive presentation is far beyond the scope of this paper. Here we will emphasize only the results from [2] and from [12], which are essential to understand our results.

2.1 Chromatic Redundancy in Natural Images

Buchsbaum and Gottshalk approached in [2] the problem of finding uncorrelated color features from a purely theoretical point of view.

They considered the abstract ensemble of all possible visual stimuli (radiances), i.e. $\mathcal{S} \equiv \{S(\lambda),\ \lambda \in \mathcal{L}\}$, where $\mathcal{L}$ is the spectrum of visible wavelengths, and built the three cone activation values as follows: $L = \int_{\mathcal{L}} S(\lambda)L(\lambda)\,d\lambda$, $M = \int_{\mathcal{L}} S(\lambda)M(\lambda)\,d\lambda$, $S = \int_{\mathcal{L}} S(\lambda)S(\lambda)\,d\lambda$.

Assuming that the stimulus $S(\lambda)$ (coming from a fixed point $\bar{x}$ of a scene) is a random variable, the *chromatic covariance matrix* associated to the three random variables L, M, S is:

$$C = \begin{bmatrix} C_{LL} & C_{LM} & C_{LS} \\ C_{ML} & C_{MM} & C_{MS} \\ C_{SL} & C_{SM} & C_{SS} \end{bmatrix}, \tag{1}$$

where $C_{LL} \equiv \mathbb{E}[L \cdot L] - (\mathbb{E}[L])^2$, $C_{LM} \equiv \mathbb{E}[L \cdot M] - \mathbb{E}[L]\mathbb{E}[M] = C_{ML}$, and so on, $\mathbb{E}$ being the expectation operator.

Let $K(\lambda,\mu) = \mathbb{E}[S(\lambda)S(\mu)] - \mathbb{E}[S(\lambda)]\cdot\mathbb{E}[S(\mu)]$ be the *covariance function*, then $C_{LL} = \iint_{\mathcal{L}^2} K(\lambda,\mu)L(\lambda)L(\mu)\,d\lambda d\mu$, and so on. To be able to perform explicit calculations, the analytical form of $K(\lambda,\mu)$ must be specified. In the absence of a database of multispectral images, Buchsbaum and Gottschalk used abstract non-realistic data to compute $K(\lambda,\mu)$. They chose the easiest covariance function corresponding to monochromatic visual stimuli, i.e. $K(\lambda,\mu) = \delta(\lambda-\mu)$, δ being the Dirac distribution.

With this choice, the entries of the covariance matrix C are all positives and they can be written as $C_{LL} = \int_{\mathcal{L}} L^2(\lambda)\,d\lambda$, $C_{LM} = \int_{\mathcal{L}} L(\lambda)M(\lambda)\,d\lambda$, and so on. C is also real and symmetric, so it has three positive eigenvalues $\lambda_1 \geq \lambda_2 \geq \lambda_3$ with corresponding eigenvectors $\mathbf{v}_i$, $i = 1,2,3$. If W is the matrix whose columns are the eigenvectors of C, i.e. $W = [\mathbf{v}_1|\mathbf{v}_2|\mathbf{v}_3]$, then the diagonalization of C is given by $\Lambda = W^tCW = \text{diag}(\lambda_1,\lambda_2,\lambda_3)$.

The eigenvector transformation of the cone excitation values L, M, S, in the special case of monochromatic stimuli, is then

$$\begin{pmatrix} A(\lambda) \\ P(\lambda) \\ Q(\lambda) \end{pmatrix} = W^t \begin{pmatrix} L(\lambda) \\ M(\lambda) \\ S(\lambda) \end{pmatrix}.$$

The transformed values A, P, Q are *uncorrelated* and their covariance matrix is Λ. A is the achromatic channel, while P and Q are associated to the opponent chromatic channels.

The *key point* in Buchsbaum and Gottschalk's theory is the application of *Perron-Frobenius theorem* (see e.g. [1] for more details), which assures that positive matrices, i.e. matrices whose entries are all strictly greater than zero, have one and only one eigenvector whose entries have all the positive sign, and this eigenvector corresponds to the largest eigenvalue, i.e. λ_1. So, only the transformed A channel will be a linear combination of the cone activation values L, M, S with positive coefficients, while the channels P and Q will show opponency. This is the theoretical reason underlying the evidence of post-retinal chromatic opponent behavior, following Buchsbaum and Gottschalk.

2.2 Spatio-chromatic Redundancy in Natural Images

The most influential paper in the analysis of spatio-chromatic redundancy is [12], where Ruderman, Cronin and Chiao proposed a *patch-based* spatio-chromatic coding and tested Buchsbaum-Gottschalk's theory on a database of 12 multispectral natural images of *foliage*.

The authors studied these LMS data built thanks to this database by first taking their decimal logarithm and then subtracting their average logarithmic value, building the so-called *Ruderman-Cronin-Chiao coordinates*, i.e. $\tilde{L} = \text{Log}\,L - \langle \text{Log}\,L\rangle$, $\tilde{M} = \text{Log}\,M - \langle \text{Log}\,M\rangle$ and $\tilde{S} = \text{Log}\,S - \langle \text{Log}\,S\rangle$. This transform is motivated with the fact that, following Weber-Fechner's law, uniform logarithmic changes in stimulus intensity tend to be equally perceptible, see [5]. Moreover, second-order statistics of log-transformed data is similar to that of linear images, see [11]. Instead, the motivation for the average substraction is to assess the data independently on the illumination level, analogously to a von Kries procedure (see [7]).

Following [12], if $\tilde{L}$, $\tilde{M}$, $\tilde{S}$, are the basis vectors in the logarithmically-transformed space, then the application of the PCA gives the following three principal axes $l = \frac{1}{\sqrt{3}}(\tilde{L} + \tilde{M} + \tilde{S})$, $\alpha = \frac{1}{\sqrt{6}}(\tilde{L} + \tilde{M} - 2\tilde{S})$, $\beta = \frac{1}{\sqrt{2}}(\tilde{L} - \tilde{M})$.

The color space spanned by these three principal axes is called $l\alpha\beta$ *space*.

To study spatiochromatic decorrelated features, Ruderman, Cronin and Chiao considered 3×3 patches, with each pixel containing a 3-vector color information, so that every patch is converted in a vector with 27 components that they analyzed with the PCA. The principal axes of these small patches in the logarithmic space are depicted in the figure at page page 2041 in [12]. The first principal axis shows fluctuations in the achromatic channel, followed by blue-yellow fluctuations in the α direction and red-green ones in the β direction.

The spatial axes are largely symmetrical and can be represented by Fourier features, in line with the translation-invariance of natural images, as argued in [3]. No pixel within the patches appear other than the primary gray, blue-yellow or red-green colors, i.e. no mixing of l, α, β has been found in any 3×3 patch. These means that not only the single-pixel principal axes l, α, β, but also the spatially-dependent principal axes $l(x), \alpha(x), \beta(x)$, viewed as functions of the spatial coordinate x inside the patches, are decorrelated.

These results have been confirmed by [8] and, in Section 4, we will perform similar experiments on much larger databases.

3 Relationship Between Second Order Stationarity and the Decorrelated Spatiochromatic Features of Natural Images

In this section we will analyze the consequence of second order stationarity in natural images on their decorrelated spatiochromatic features, by first considering gray-level images, where stationarity implies that the principal components are Fourier basis functions, then extending this result to the color case. The supplementary hypothesis on color covariance matrices will yields principal components given by the tensor product between Fourier basis functions and achromatic plus opponent color coordinates.

3.1 The Gray-Level Case

Let I be a gray-level natural image of dimension $W \times H$, W being the width (number of columns) and H being the height (number of rows) of I.

If we denote the H rows of I as $r^0, \dots, r^{H-1}$, then we can describe the position of each pixel of I row-wise as follows:

$$I = \{r_k^j;\ j = 0, \dots, H-1,\ k = 0, \dots, W-1\}, \tag{2}$$

j is the row index and k is the column index. Each row $r^j = (r^j_0, \ldots, r^j_{W-1})$ will be interpreted as a W-dimensional random vector and each component r^j_k as a random variable.

Let us define the *spatial covariance of the two random variables* r^j_k, $r^{j'}_{k'}$:

$$\text{cov}(r^j_k, r^{j'}_{k'}) \equiv c^{j,j'}_{k,k'} = \mathbb{E}[r^j_k r^{j'}_{k'}] - \mathbb{E}[r^j_k]\mathbb{E}[r^{j'}_{k'}]. \tag{3}$$

Due to the symmetry of covariance we have $c^{j,j'}_{k,k'} = c^{j',j}_{k',k}$. Then, we can write the *spatial covariance matrix of the two random vectors* r^j, $r^{j'}$ as $\text{cov}(r^j, r^{j'}) \equiv C^{j,j'}$ and the *spatial covariance matrix* C of the image I, respectively, as follows:

$$C^{j,j'} = \begin{bmatrix} c^{j,j'}_{0,0} & c^{j,j'}_{0,1} & \cdots & c^{j,j'}_{0,W-1} \\ c^{j,j'}_{1,0} & c^{j,j'}_{1,1} & \cdots & c^{j,j'}_{1,W-1} \\ \vdots & \vdots & \ddots & \vdots \\ c^{j,j'}_{W-1,0} & \cdots & \cdots & c^{j,j'}_{W-1,W-1}, \end{bmatrix} \tag{4}$$

$C = (C^{j,j'})_{j,j'=0,\ldots,H-1}$. Notice that C is a $HW \times HW$ matrix because each sub-matrix $C^{j,j'}$ is a $W \times W$ matrix.

Hypothesis 1. From now on, the covariance of I is assumed to be invariant under translations of the row and column index: $c^{j,j'}_{k,k'} = c^{|j-j'|}_{|k-k'|}$.

Hypothesis 1 will be tested in Section 4. We notice that it is weaker than the typical definition of second order stationarity because here we do not assume the translation invariance of the mean.

Alongside this hypothesis, we add the typical requirement of *symmetrized spatial domain with a toroidal distance* implicitly assumed in the Fourier contest, i.e. $r^j_k = r^{j'}_{k'}$ when $j \equiv j' \pmod{H}$ and $k \equiv k' \pmod{W}$.

Noticing that $c^{j,j'}_{k,k'} = c^{j,j'}_{k+1,k'+1}$, we have that the $C^{j,j'}$ are *circulant matrices*, i.e. matrices where each row vector is rotated one element to the right relative to the preceding row: $C^{j,j'} = \text{circ}\left(c^{j,j'}_{0,0}, c^{j,j'}_{0,1}, \ldots, c^{j,j'}_{0,W-1}\right)$.

Now, writing $C^j \equiv C^{0,j}$, $j = 0, \ldots, H-1$ it is straightforward to see that C is block-circulant: $C = \text{circ}\left(C^0, C^1, \ldots, C^{H-1}\right)$.

Thanks to the well known relationship between circulant matrices and discrete Fourier transform (DFT), see e.g. [4], the eigenvectors of the matrices C^j are the Fourier basis vectors: $\mathbf{e}_m = \frac{1}{\sqrt{W}}\left(1, e^{-\frac{2\pi i m}{W}}, \ldots, e^{-\frac{2\pi i m(W-1)}{W}}\right)^t$ and their eigenvalues are given by components of the DFT of the first row of C^j: $\hat{c}^{0,j}_{0,m} = \sum_{k=0}^{W-1} c^{0,j}_{0,k} e^{-\frac{2\pi i m k}{W}}$.
The set of eigenvalue equations $C^j \mathbf{e}_m = \lambda^j_m \mathbf{e}_m$, can be written as the following matrix equation $C^j E_W = \Lambda^j E_W$, where $\Lambda^j = \text{diag}(\hat{c}^{0,j}_{0,m};\ m = 0, \ldots, W-1)$ and E_W are the Vandermonde matrices:

$$E_W = \frac{1}{\sqrt{W}} \begin{bmatrix} 1 & 1 & \cdots & 1 \\ 1 & e^{-\frac{2\pi i}{W}} & \cdots & e^{-\frac{2\pi i(W-1)}{W}} \\ \vdots & \vdots & \ddots & \vdots \\ 1 & e^{-\frac{2\pi i(W-1)}{W}} & \cdots & e^{-\frac{2\pi i(W-1)^2}{W}} \end{bmatrix}. \tag{5}$$

Notice now that if we have a block-circulant matrix $M = \text{circ}(M^0, \dots, M^{H-1})$ with the property that the blocks M^j can be diagonalized on the same basis B, then it can be verified by direct computation that $E_H \otimes B$ is a basis of eigenvectors of M, where $\otimes$ denotes the Kronecker product and $E_H = [\mathbf{e}_0|\mathbf{e}_1|\cdots|\mathbf{e}_{H-1}]$.

In the case of our spatial covariance matrix C, all the submatrices C^j have the same basis of eigenvectors E_W, thus, if we define $E_H \otimes E_W = [\mathbf{e}_{m,l}]$ as $\mathbf{e}_{m,l} = \left(1, e^{-2\pi i(\frac{m}{W}+\frac{l}{H})}, \dots, e^{-2\pi i(\frac{m(W-1)}{W}+\frac{l(H-1)}{H})}\right)^t / \sqrt{HW}$, for $m = 0, \dots, W-1$, and $l = 0, \dots, H-1$, then $E_H \otimes E_W$ provides a basis of eigenvectors for C. Actually, due to the symmetry of covariance matrices, the complex parts of the exponentials involving the sinus function cancel out (see [6]) and so the 2D cosine Fourier basis also constitutes a basis of eigenvectors of C.

3.2 The Color Case

Let $\mathbf{u} : \Omega \to [0, 255]^3$ be an RGB image function, where Ω is the spatial domain, and, for all $(j, k) \in \Omega$, $\mathbf{u}(j, k) = (R(j, k), G(j, k), B(j, k))$ is the vector whose components are the red, green and blue intensity values of the pixel defined by the coordinates (j, k).

We define the *spatiochromatic covariance matrix among two pixels of position* (j, k) *and* (j', k') by extending eq. (3) as follows $c^{j,j'}_{k,k'}(R, G, B)$

$$\begin{bmatrix} C_{RR}(j,j',k,k') & C_{RG}(j,j',k,k') & C_{RB}(j,j',k,k') \\ C_{GR}(j,j',k,k') & C_{GG}(j,j',k,k') & C_{GB}(j,j',k,k') \\ C_{BR}(j,j',k,k') & C_{BG}(j,j',k,k') & C_{BB}(j,j',k,k') \end{bmatrix}. \tag{6}$$

In the particular case defined by $j' = j$ and $k' = k$, we will call $c^{j,j'}_{k,k'}(R, G, B)$ '*chromatic autocovariance*' and denote it simply as $c^0(R, G, B)$. By substituting $c^{j,j'}_{k,k'}$ with $c^{j,j'}_{k,k'}(R, G, B)$ in the matrices appearing in (4), we find the *spatiochromatic covariance matrix* $C^{j,j'}(R, G, B)$ *among the two random vectors* r^j, $r^{j'}$ and the *spatiochromatic covariance matrix* $C(R, G, B)$ *of the RGB image* u, which is a $3HW \times 3HW$ matrix.

Now, supposing that all the elements of the matrices (6) are positive, thanks to the Perron-Frobenius theorem we can assure that each of these $c^{j,j'}_{k,k'}(R, G, B)$ matrices has a basis of eigenvectors that can be written as a triad of achromatic plus opponent chromatic channels. If we further *assume that the matrices (6) can be diagonalized on the same basis of eigenvectors* (A, P, Q), then, thanks to what remarked before, the eigenvectors of the spatiochromatic covariance matrix $C(R, G, B)$ can be written as the Kronecker product: $(A, P, Q) \otimes \mathbf{e}_{m,l} \in \mathbb{R}^{3HW}$, which is precisely the type of eigenvectors that have been exhibited experimentally in [10]. A standard result of linear algebra guarantees that a set of matrices can be diagonalized on the same basis of eigenvectors if and only if they commute[1]. Thanks to the hypothesis of translation invariance of covariance, this is verified if and only if the generic covariance matrix $c^{j,j'}_{k,k'}(R,G,B)$ commutes with the chromatic autocovariance matrix $c^0(R,G,B)$.

It is convenient to resume all the hypotheses made and results obtained so far in the following proposition.

Proposition 1. *Let* $\boldsymbol{u} : \Omega \to [0,255]^3$ *be an RGB image function, with a periodized spatial domain* Ω*, and suppose that:*

1. *The spatiochromatic covariance matrices matrices* $c^{j,j'}_{k,k'}(R,G,B)$ *defined in (6) depend only on the distances* $|j-j'|$, $|k-k'|$, *i.e. the covariance of* $\boldsymbol{u}$ *is stationary;*
2. *All matrices* $c^{j,j'}_{k,k'}(R,G,B)$ *are positive, i.e. their elements are strictly greater than 0;*
3. *The following commutation property holds:*

$$[c^0(R,G,B), c^{j,j'}_{k,k'}(R,G,B)] = 0, \;\; \forall (j,k),(j',k') \in \Omega. \tag{7}$$

Then, the eigenvectors of the spatiochromatic covariance matrix $C(R,G,B)$ *can be written as the Kronecker product* $(A,P,Q) \otimes \boldsymbol{e}_{m,l}$*, where* (A,P,Q) *is the achromatic plus opponent color channels triad and* $\boldsymbol{e}_{m,l}$ *is the 2D cosine Fourier basis.*

Proposition 1 defines a mathematical framework where the empirical result shown in [12] can be formalized and understood in terms of statistical properties of natural images. In the following section we will test this framework with the help of two large databases of RGB images.

4 Validations on a Natural Image Database

In this section we present the tests that we have performed to check the validity of the hypotheses of Proposition 1.

To perform our numerical experiences we have generated a databases of RAW photographs made of 1746 natural scenes, available at http://download.tsi.telecom-paristech.fr/RawDatabase/. Each 4-neighborhood of pixels in a raw image contains two pixels corresponding to the R and B channels and two pixels corresponding to the G channel. We demosaicked each RAW image to build a subsampled RGB image simply by keeping unaltered the R and B information and averaging the G channel. The advantage of this database is that RAW images are free

[1] We recall that, given two generic matrices A and B for which the products AB and BA is well defined, $[A,B] \equiv AB - BA$ is called the 'commutator' between them. Of course A and B commute if and only if $[A,B] = 0$.

from post-processing operations such as gamma correction, white balance or compression, thus, modulo camera noise, they provide a much better approximation of physical irradiance than common jpeg images.

4.1 $c^0(R, G, B)$ and Its Eigenvalues and Eigenvectors

The expression of the chromatic autocovariance matrix relative to the RAW database, $c^0(R, G, B)$, is:

$$c^0(R, G, B) = \begin{bmatrix} 0.0022 & 0.0021 & 0.0021 \\ 0.0021 & 0.0021 & 0.0022 \\ 0.0021 & 0.0022 & 0.0024 \end{bmatrix} \tag{8}$$

which confirm the positivity assumption on $c^0(R, G, B)$. Its eigenvectors are:

$$\begin{cases} A = (0.5679, 0.5683, 0.5954) & \longleftrightarrow \quad \lambda_1 = 0.0065, \\ P = (0.7210, 0.0055, -0.6930) & \longleftrightarrow \quad \lambda_2 = 0.0002, \\ Q = (0.3971, -0.8228, 0.4066) & \longleftrightarrow \quad \lambda_3 = 7.8 \cdot 10^{-7}. \end{cases} \tag{9}$$

4.2 The Exponential Decay of Spatiochromatic Covariance

To simplify the notation, from now on we will write $c_{k,k'}^{j,j'}(R, G, B) \equiv c^d(R, G, B)$, where d is the Euclidean distance between (j, k) and j', k'. All the spatiochromatic matrices $c^d(R, G, B)$ that we have estimated turned out to be *positive*. Their decay with respect to increasing values of d is reported in semi-logarithmic scale in Fig. 1 for the Flickr and the RAW database, respectively.

The graphs of Fig. 1 show a linear decay for all the distances that we have tested (from 1 to 300 pixels) quantified by a coefficient of determination R^2 greater than 0.98 for all curves.

Let us now write the generic element of the matrix $c^d(R, G, B)$ as $c_{\mu\nu}^d$, $\mu, \nu \in \{R, G, B\}$. A linear behavior in the semilogarithmic domain corresponds the following exponential decay: $c_{\mu\nu}^d = c_{\mu\nu}^0 e^{\beta_{\mu\nu} d}$, $\mu, \nu \in \{R, G, B\}$, where $c_{\mu\nu}^0$ is the generic element of the chromatic autocovariance matrix and $\beta_{\mu\nu} < 0$.

The value of the coefficients $\beta_{\mu\nu}$ (i.e. the slopes of the straight lines which approximate the spatiochromatic covariance graphs in the semilogarithmic scale) are the following: $\beta_{RR} = -0.0023$, $\beta_{GG} = -0.0021$ $\beta_{BB} = -0.0020$ $\beta_{RG} = \beta_{GR} = -0.0022$ $\beta_{RB} = \beta_{BR} = -0.0022$ $\beta_{GB} = \beta_{BG} = -0.0021$.

It can be seen that the spatiochromatic covariance relative to the blue channel decreases less rapidly than that of the red and green channels. This may be explained by the fact that pictures in which the sky is present are characterized by large homogeneous areas dominated by the blue channel.

The explicit analytical expressions of $c^d(R, G, B)$ obtained provide an accurate model for the covariance that corrects the power-law decay. Moreover, they allow computing the commutators $[c^0(R, G, B), c^d(R, G, B)]$ for every distance $d > 0$. If the coefficients $\alpha_{\mu\nu}$ were all perfectly equal, then these commutators

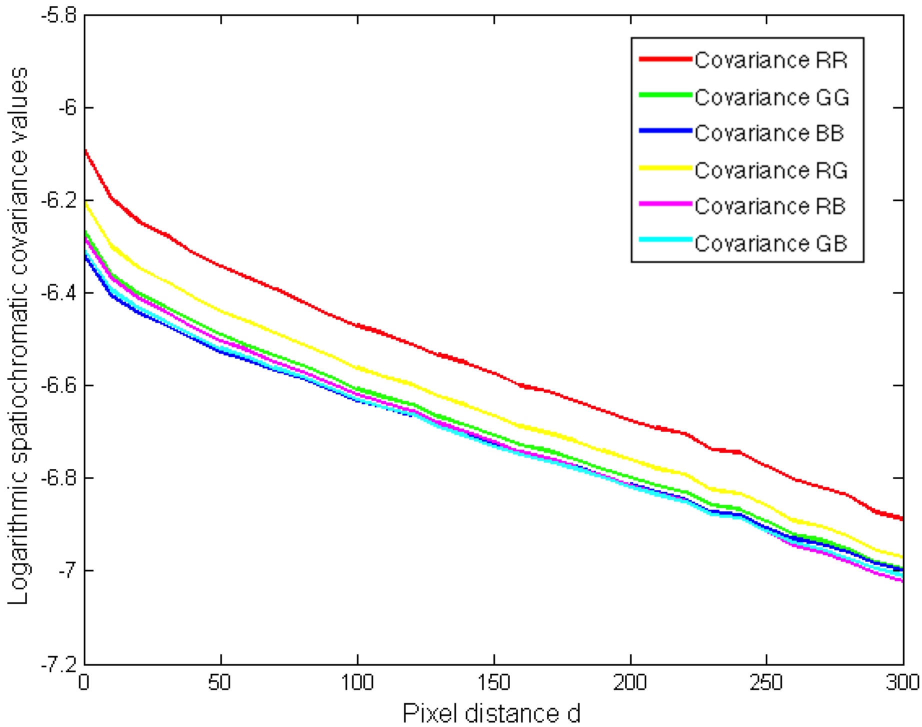

Fig. 1. The linear behavior of the six spatiochromatic covariance matrix elements in the semi-logarithmic scale as a function of d, which implies an exponential decay.

would be exactly null matrices, however, the differences in the values of the exponentials make the matrix elements of the commutators slightly different than zero. Nonetheless the highest deviation from the zero matrix that we have found can be quantified with a matrix norm of $4.5 \cdot 10^{-7}$, thus showing that the commutation hypothesis is verified with very good precision.

In proposition 1, the hypothesis of commutativity is essential to guarantee that the spatiochromatic covariance matrices can be diagonalized on the same basis of eigenvectors.

5 Discussion and Perspectives

We have provided a theoretical analysis of the relationship between translation invariance of the covariance and the decorrelated spatiochromatic features of digital RGB images, supported by several numerical tests.

Our analysis has been motivated by the will to understand the basic mathematical reasons underlying the appearance of a separable spatiochromatic basis of uncorrelated features when the PCA is performed over patches or whole natural images.

In order to investigate this property, we have built the spatiochromatic covariance matrix of an abstract three-chromatic image and we have shown that, under the assumption of spatial invariance and commutativity, their eigenvectors can be written as the Kronecker product of the cosine Fourier basis times an achromatic plus color opponent triad.

The numerical tests that we have conducted have shown that the assumptions are verified with a good degree of approximation on a quite large database of RAW images.

In particular, the analysis of the commutativity of spatiochromatic covariance matrices have led to a lateral result that it is worth underlying: our tests have shown that the spatial covariance decays exponentially and not following a power law. The failure of the power law decay has already been reported in the literature of natural image statistics, but our result on the exponential decay is novel. Moreover, we have shown that the decay speed is not the same for all the combinations of chromatic channels: the autocovariance decay of the blue channel being the slowest and the R-B covariance decay being the fastest.

References

1. Berman, A., Plemmons, R.: Nonnegative Matrices in the Mathematical Sciences. SIAM (1987)
2. Buchsbaum, G., Gottschalk, A.: Trichromacy, opponent colours coding and optimum colour information transmission in the retina. Proc. Royal Society of London B **220**, 89–113 (1983)
3. Field, D.: Relations between the statistics of natural images and the response properties of cortical cells. J. Opt. Soc. Am. **4**(12), 2379–2394 (1987)
4. Frazier, M.W.: Introduction to wavelets through linear algebra. Springer (2001)
5. Goldstein, B.: Sensation and Perception, 9th edn. Cengage Learning (2013)
6. Gray, R.: Toeplitz and Circulant Matrices: A review. Now Publishers Inc. (2006)
7. von Kries, J.: Chromatic adaptation. Festschrift der Albrecht-Ludwigs-Universität, pp. 145–158 (1902)
8. Párraga, C., Troscianko, T., Tolhurst, D.: Spatiochromatic properties of natural images and human vision. Current Biology **6**(12), 483–487 (2002)
9. Provenzi, E., Delon, J., Gousseau, Y., Mazin, B.: Second order stationarity and spatiochromatic properties of natural images. In: 2014 Tenth International Conference on Signal-Image Technology and Internet-Based Systems (SITIS), November 23–27, Marrakech, pp. 598–605. IEEE (2014)
10. Ruderman, D.: Origin of scaling in natural images. Vision Research **37**, 3385–3398 (1996)
11. Ruderman, D., Bialek, W.: Statistics of natural images: Scaling in the woods. Phys. Rev. Lett. **73**, 814–817 (1994)
12. Ruderman, D., Cronin, T., Chiao, C.: Statistics of cone responses to natural images: implications for visual coding. J. Opt. Soc. Am. A **15**(8), 2036–2045 (1998)